

Modeling Soil Moisture, Water Partitioning, and Plant Stress under Irrigated Conditions in Desert Urban Areas

Thomas J. Volo

M.S. Student, School of Sustainable Engineering and the Built Environment

Enrique Vivoni (project advisor)

Associate Professor, School of Sustainable Engineering and the Built Environment
& School of Earth and Space Exploration

Chris A. Martin (collaborator)

Professor, School of Letters and Sciences

Stevan Earl (collaborator)

CAP LTER Site Manager, Global Institute of Sustainability

Arizona State University

Submitted to CAP Award for Water Research

April 8, 2013

Abstract

A point-scale model of soil moisture dynamics is applied to two different urban landscape designs in the Phoenix, AZ metropolitan area: a xeriscaped site (gravel base and low water-use plants), and a mesiscaped site (turf grass and shade trees). The model is calibrated to observed soil moisture data from a sensor at the xeric site with no anthropogenic water input, as well as irrigated sensors at both sites, using local meteorological records as model forcing. Experiments are then run using the calibrated model at both irrigated sites to investigate the effects of irrigation scheduling, plant stress characteristics, and inter- and intra-annual variability of precipitation on soil moisture dynamics, water partitioning, and plant water stress.

Calibration results include a substantial difference in storage capacity at the two sites primarily due to differences in the depth of the rooting zone; this affects the applicability of different irrigation schedules at the two sites. At the xeric site, seasonal variation of irrigation input is shown to be highly important to avoid losses to deep infiltration beyond the rooting zone while simultaneously maintaining plant health. At the mesic site, seasonal variation is less important, though water savings may be achieved under certain circumstances using large infrequent irrigation pulses, as opposed to daily applications of smaller volumes. A final analysis determines the monthly minimum water input required to achieve specified levels of stress tolerance at both sites, using several decades of precipitation and potential evapotranspiration data.

These types of analyses are intended to assist water and landscape managers in developed desert and semiarid areas, by identifying opportunities for water savings and assessing the benefits and drawbacks of xeriscaped landscaping and flood-style irrigation, based on a quantitative model that incorporates local soil, vegetation, and climatic parameters.

1. Introduction

Native and exotic tree, shrub, and grass species are utilized in urban areas for shade, recreation, pollution reduction, and aesthetics. However, they are often dependent upon and highly responsive to supplemental water supplies beyond precipitation and groundwater stores, particularly in desert and semiarid conditions. Despite the highly engineered nature of urban water systems, and the substantial role that irrigation plays on plant conditions in developed areas, there is still a great need for a better understanding of the fate of water used to maintain municipal and residential landscapes (Pataki *et al.*, 2011). The coupled relationship between water and energy balances magnifies the importance of an improved comprehension of water budgets, especially considering the growing use of water-sensitive urban design elements that have the potential to affect urban microclimates, in attempt to mitigate the environmental impacts of development (Mitchell *et al.*, 2010). The current demand for improved urban climate modeling (Grimmond *et al.*, 2010) must therefore be informed by a similarly improved quantitative understanding of urban water fluxes. Furthermore, while current ecohydrology literature is replete with physically-based models, it is comparatively lacking in studies that couple empirical approaches with modeling efforts, and those that include manipulative experimental design (King and Caylor, 2011). Thus, this study, which utilizes data from designed plots that include irrigated urban vegetation, is motivated by shortages in the literature both in content and in method, with a goal of aiding in landscape management and design through a more complete understanding of the budgets of urban landscape irrigation.

While the factors that influence plant water use and uptake in urban settings are not currently understood completely, plant-available soil moisture is clearly a major driver for the viability of exotic plant species in urban landscapes (McCarthy and Pataki, 2010). However, in order to maintain sufficient soil moisture levels to reap the benefits of urban vegetation, several tradeoffs must be considered, including additional plant maintenance, capital outlay for irrigation systems at both the individual and state or municipal level, and the ongoing direct costs of water supply, especially in areas where sources are limited. Nonetheless, outdoor water use (including use for swimming pools) comprises greater than 50% of residential water consumption (Mayer and DeOreo, 1999). Furthermore, though annual water use has been shown to be sensitive to seasonal climate patterns (Balling and Gober, 2007), residential irrigation specifically is relatively insensitive to climate, since adjustments to automated irrigation systems are rarely made often enough to appropriately respond to fluctuations in evapotranspiration and precipitation (Martin, 2001). Irrigation is thus frequently in excess of plant demand, resulting in a potential for substantial water conservation through landscape irrigation with water budgets based on plant demands and potential evapotranspiration (White *et al.*, 2004).

These issues are particularly pertinent in the Phoenix, Arizona metropolitan area, where natural and anthropogenic factors have combined to make the region a worthwhile case study in several branches of sustainability science. Arising from the inland Sonoran Desert and totaling over 4 million inhabitants, the metropolis consisting of Phoenix, Mesa, Chandler, Glendale, Scottsdale, Gilbert, Tempe, and the surrounding municipalities primarily receives its water from upstream basins along the Salt, Verde, and (through the Central Arizona Project canal system) Colorado Rivers (City of Phoenix, 2011). Despite this lack of local water sources, per capita consumption and outdoor use in particular far surpass rates in other urban centers, making water conservation a primary concern as populations are expected to double in the coming decades (Balling *et al.*, 2008). Landscape designs that reflect the natural desert ecology have been shown to require less water input than exotic turf grass lawns (Martin, 2008), but there is strong societal resistance to such xeriscaped design, related to individual value judgments on aesthetics, safety, maintenance, and the very concept of the desert as “home” (Larson *et al.*, 2009). Additionally, though xeriscaping has the potential to mitigate urban heat island effects that have been documented in the Phoenix area for decades, thermal discomfort and net warming have been shown to increase with a shift from grass lawns (mesic) to desert (xeric) landscape designs (Chow and Brazel, 2012). These environmental, economic, and social impacts that can occur due to changes in landscape design underscore the importance of a greater understanding of the hydrological differences between design modes.

In this study, we apply a quantitative, physically-based model of soil moisture dynamics that includes variations in potential evapotranspiration to an experimental site in Mesa, Arizona that includes irrigation of both mesic and xeric urban landscapes. After calibrating the model to observed data, we analyze potential irrigation patterns in terms of relative soil moisture, water fate, and plant water stress, as well as the impacts of inter- and intra-annual variability in precipitation on plant stress under irrigated conditions at both sites. Finally, for each site and according to the climate history of the area over several decades, irrigation schedules are designed that minimize water use while avoiding both inelastic plant response to moisture shortages and overproduction of biomass.

2. Methods

2.1 Soil Moisture Model

As illustrated in Figure 1, the conceptual model used is centered on interactions affecting the soil water balance. Soil and vegetative characteristics control the impact of meteorological forcing on water fluxes, then factor into the determination of plant water stress from the resultant soil moisture values. Irrigation is modeled as an additional forcing element, independent of, but supplemental to, precipitation input. Soil moisture dynamics are simulated mathematically, based on a point-scale model proposed by Laio *et al.* (2001b), but including an additional term to account for anthropogenic water input. Furthermore, historical precipitation data are used to test the model against soil moisture observations, as opposed to the stochastic rainfall input included by the model's original authors to facilitate their probabilistic approach.

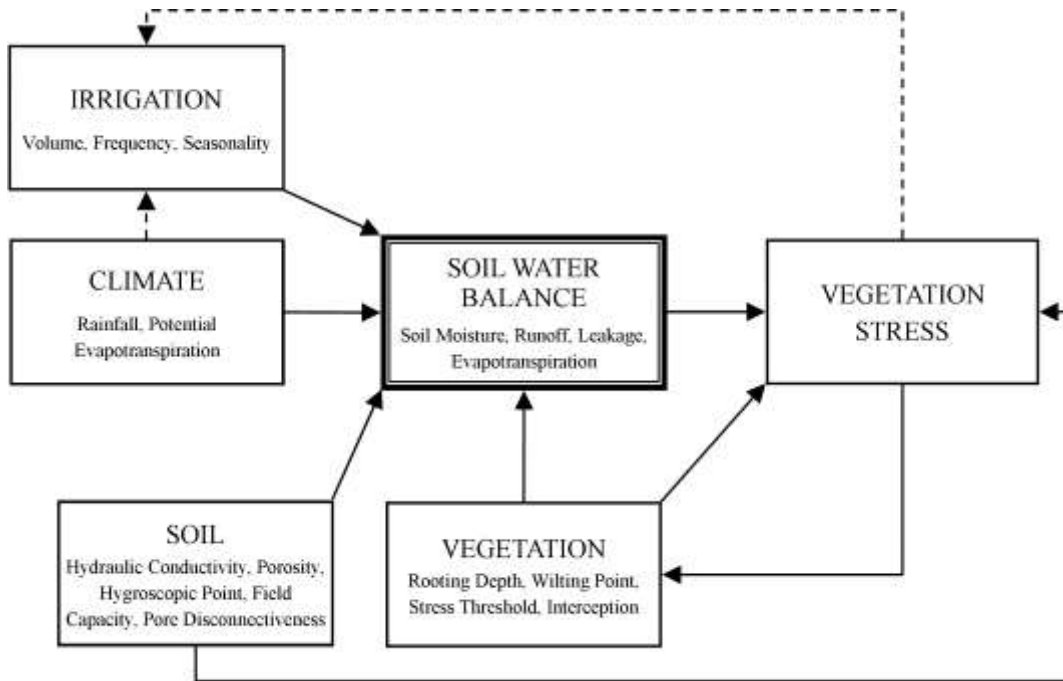


Figure 1. Conceptual schematic of modeled system. Solid lines show modeled interactions; dotted lines represent secondary interactions not directly considered. (Adapted from Rodriguez-Iturbe *et al.*, 2001)

In the following equation, the change in relative soil moisture s (dimensionless, 0 for perfectly dry soil and 1 at saturation) is expressed as the result of applicable water fluxes, averaged over a rooting depth Z_r [L]:

$$nZ_r \frac{ds}{dt} = P + I - ET(s) - L(s) - Q(s), \quad (1)$$

with soil porosity n [-], precipitation P , irrigation I , evapotranspiration ET , leakage L , and runoff Q (all [$L T^{-1}$]). A numerical approach is applied, discretizing the above differential equation at a daily time scale. For each time step, water inputs ($P + I$) are added to the soil moisture value from the previous time step, resulting in an intermediate s value used for the determination of water losses through ET , L and Q .

Evapotranspiration is treated as a multi-stage function of relative soil moisture, with the boundaries between behaviors delineated by threshold values determined by soil and vegetation properties.

$$ET(s) = \begin{cases} 0 & s \leq s_h \\ \frac{s - s_h}{s_w - s_h} E_w & s_h \leq s \leq s_w \\ E_w + \frac{s - s_w}{s^* - s_w} (ET_{max} - E_w) & s_w \leq s \leq s^* \\ ET_{max} & s \geq s^*. \end{cases} \quad (2)$$

The hygroscopic point s_h and field capacity s_{fc} are related to matric potentials through a soil's water retention curve and are dependent only on soil characteristics (Clapp and Hornberger, 1978). E_w , the rate of evaporation from bare soil below the wilting point is similarly dependent only on soil characteristics, though the wilting point s_w and stress threshold s^* are additionally dependent on vegetation (Laio *et al.*, 2001b). Potential evapotranspiration (PET) as determined by the Penman-Monteith equation is used as the maximum rate of evapotranspiration ET_{max} , a possibility suggested by Laio *et al.* (2001b), and utilized by Caylor *et al.* (2005). Additionally, the use of ET values calculated from daily observations, as opposed to temporally invariant or seasonal estimates (e.g. Caylor *et al.*, 2005; Laio *et al.*, 2004; Porporato *et al.*, 2003), is a further refinement to the originally proposed model added to more accurately reflect soil moisture dynamics while taking advantage of available data.

Leakage, or deep infiltration beyond the active rooting zone, is assumed to only occur when relative soil moisture s surpasses the field capacity of the soil s_{fc} . The leakage rate L is modeled as a fraction of the saturated hydraulic conductivity K_s [$L T^{-1}$], and is a function of s , dependent on only soil (i.e. not vegetative) parameters:

$$L(s) = K_s \frac{e^{\beta(s-s_{fc})} - 1}{e^{\beta(1-s_{fc})} - 1}, \quad (3)$$

where $\beta = 2b + 4$ and b [-] is the pore size distribution index. Thus the hydraulic conductivity decays exponentially from a maximum at the saturated value when $s = 1$, to zero when $s = s_{fc}$.

Runoff Q is only modeled as being generated through saturation excess (Dunne runoff mechanism), i.e. when the application of water inputs (rainfall plus irrigation) results in values for s greater than 1. In these cases, the depth of water input attributed to runoff is calculated as $nZ_r(s - 1)$, thereby returning s to the level of saturation for subsequent calculations. While other studies (e.g. Manfreda *et al.*, 2010) have investigated the impact of including infiltration excess (Hortonian) runoff, preliminary results indicated that soil permeabilities in this study were sufficiently high to allow for the exclusion of such effects without significant change to modeled soil moisture values, water partitioning, or vegetation stress levels.

Plant water stress $\zeta(s)$ is calculated in relation to s^* , at which stomatal closure is induced ($\zeta = 0$), and the wilting point s_w , at which transpiration ceases ($\zeta = 1$).

$$\zeta(s) = \left(\frac{s^* - s}{s^* - s_w} \right)^q. \quad (4)$$

In this function of static water stress proposed by Porporato *et al.* (2001), q represents the ability of a plant to withstand low levels of water stress with minimal physiological response while reserving more drastic and potentially inelastic response for periods of greater water stress (Rodriguez-Iturbe and Porporato, 2004). Proposed by the same authors, a function for mean dynamic water stress $\bar{\theta}$ totaled over a growing season T_{seas} is used to quantify the effects of prolonged exposure to moisture conditions below the stress threshold:

$$\bar{\theta} = \begin{cases} \left(\frac{\bar{\zeta}' \bar{T}_{s^*}}{k T_{seas}} \right)^{1/\sqrt{\bar{n}_{s^*}}} & \text{if } \bar{\zeta}' \bar{T}_{s^*} < k T_{seas}, \\ 1 & \text{otherwise.} \end{cases} \quad (5)$$

Here, \bar{n}_{s^*} is the average number of periods in a growing season with $s < s^*$, and \bar{T}_{s^*} and $\bar{\zeta}'$ are, respectively, the average duration and intensity of these periods. k represents the ability of a plant to withstand and potentially adapt to periods of prolonged water stress; it can be seen as the maximum average ζ value a plant can endure for an entire growing season without permanent damage. Due to the year-round warm temperatures of the region, a growing season of 1 year is assumed.

2.2 Study Site

Funded by the Central Arizona-Phoenix Long-Term Ecological Research Project (CAP LTER), the North Desert Village landscape experiment (NDV) is located on the Arizona State University Polytechnic Campus in Mesa, Arizona (33.31° N, 111.68° W, elevation 406 m). The campus lies near the eastern edge of the greater Phoenix metropolitan area, which is surrounded by the Sonoran Desert (Figure 2a-c). Average daily maximum temperatures in the area range from 19° C (66° F) in December to 42° C (104° F) in July, with an average 175 days per year above 32° C (90° F), occasionally surpassing 46° C (115° F) in the summer months. Rainfall averages ~250 mm annually, arriving predominantly by winter storms (December-February, 45% of total annual rainfall) and late summer monsoon and thunderstorm activity (July-September, 30%), with little to no precipitation in spring and early summer months (March-May, 15%; June, <1%). (Climate statistics compiled from the National Climatic Data Center, www.ncdc.noaa.gov, East Mesa location, 2002-2011.) Annual PET rates in the area average ~2000 mm (Balling *et al.*, 2008), which are sufficiently high compared to precipitation rates to classify the area as desert conditions under the Köppen climate classification system.

In 2005, four small “neighborhoods” were fitted with differing vegetation and irrigation treatments; a fifth was maintained without any particular treatment as an experimental control. Each neighborhood consisted of six pre-existing single-story homes (100-200 m²) occupied by university faculty, staff, students, and their families. Landscape treatments were installed in the yards of each house, as well as in common areas between structures (Figure 2d, e). As detailed in Table 1, the “mesic” site includes turf grass and high water use shade trees, while the “xeric” site features a gravel base with a combination of native and exotic low water use trees and shrubs. Irrigation systems appropriate for each vegetative cover were also installed, including sprinkler systems for turf grass, and individual drip irrigators at trees and shrubs for areas with predominantly gravel cover. (Though not utilized in this study, the “native” site includes only plant species native to the surrounding Sonoran Desert without any irrigation, and the “oasis” site is dominated by gravel cover and exotic plants, but also includes small “islands” of turf grass.) Each of the four treatment areas was instrumented with two sensors measuring volumetric water content at 30 cm depth, recording at hourly intervals. Other measurements at each of the treatment sites include soil temperature, surface temperature, air temperature, and soil heat flux. Surveys have also been conducted of the residents of each neighborhood, allowing NDV to provide research

opportunities across a wide range of disciplines related to urban sustainability, including social decisions, biodiversity, and microclimate patterns.

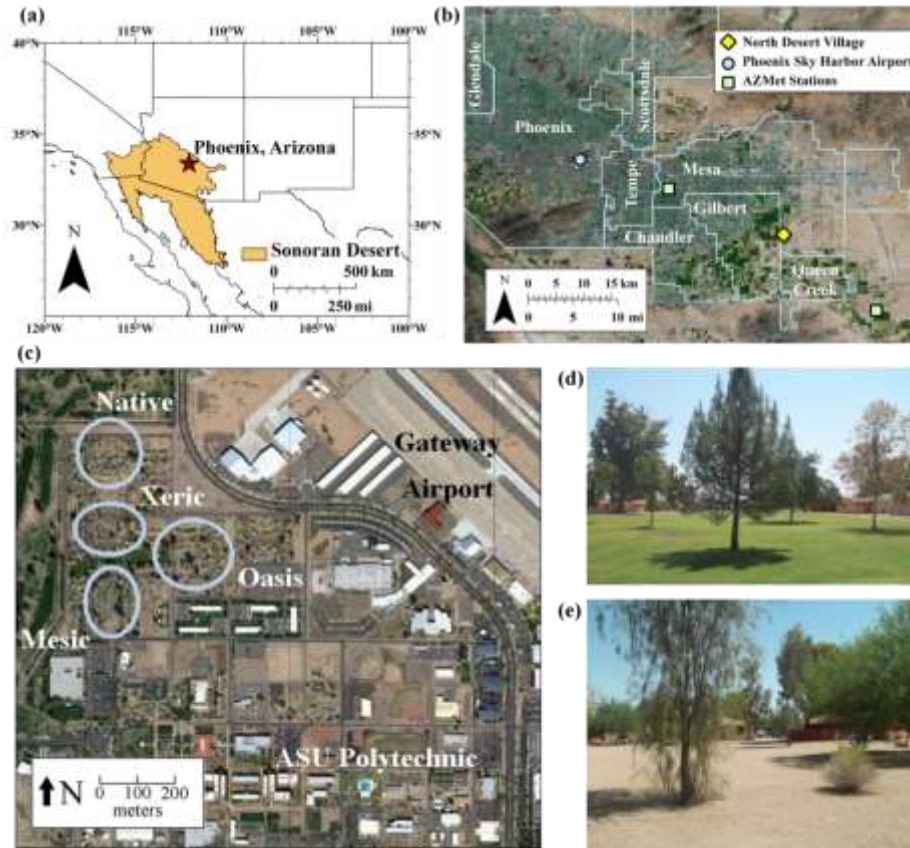


Figure 2. Location of the North Desert Village landscape experiment, with respect to (a) the southwestern United States and the Sonoran Desert and (b) the Phoenix metropolitan area. (c) Four instrumented “neighborhoods” at NDV and surrounding area. Images of the mesic (d) and xeric (e) sites. Data from the native and oasis sites were not used in this study.

Table 1. Landscape and irrigation treatments of four neighborhoods at NDV (Yabiku *et al.*, 2008).

Treatment	Ground Cover	Plant Types and Examples	Irrigation	Sensor Cover
MESIC	Turf grass	High water use shade trees and turf grass Turkish pine (<i>Pinus brutia</i>) Arizona sycamore (<i>Platanus wrightii</i>) Bermuda grass (<i>Cynodon dactylon</i>)	Sprinkler	Turf grass Turf grass
XERIC	Granitic gravel substrate	Low water use native and exotic trees Eucalyptus (<i>E. microtheca</i>) Palo verde (<i>Parkinsonia</i> hybrid) Mesquite (<i>Prosopis</i> hybrid)	Individual drip emitters at each shrub and tree	Bare soil/gravel Palo verde
OASIS	Granitic gravel substrate with turf grass “islands”	High and low water use exotic trees and shrubs European fan palm (<i>Chamaerops humilis</i>) Desert petunia (<i>Ruellia peninsularis</i>) Bermuda grass (<i>Cynodon dactylon</i>)	Sprinklers on turf grass with individual emitters in gravel areas	Turf grass Bare soil/gravel
NATIVE	Gravel	Native Sonoran Desert plants Agave (<i>A. Americana</i>) Saguaro cactus (<i>Carnegiea gigantea</i>) Creosote bush (<i>Larrea tridentate</i>)	None	Bare soil/gravel Saguaro cactus

The Soil Survey Geographic (SSURGO) database (a product of the U.S. Department of Agriculture) classifies the entirety of NDV as Mohall loam. While this study does not use soil properties or characteristics from SSURGO, the single soil classification for the entire area is used to justify the use of soil parameters calibrated at one NDV site to others within the area. The site also exhibits low relief, with variations in altitude <1 m throughout NDV. This allows an assumption of generally negligible lateral fluxes, and thus the applicability of a one-dimensional model of soil moisture dynamics.

2.3 Data

Rainfall records and daily PET values were taken from the Arizona Meteorological Network (AZMET) station at Queen Creek (see Figure 2b), approximately 20 km southeast of NDV, and supplemented by data from the AZMET station in Mesa, 20 km northwest of NDV. Hourly records were aggregated to daily data to match the time step of the numerical model. Though spatial heterogeneity of precipitation is to be expected, particularly for summer thunderstorms, the magnitude and timing of rain events between the two stations was found to be sufficiently comparable to allow an assumption of similar rainfall at NDV between them. Unfortunately, annual precipitation totals from the Phoenix-Mesa Gateway Airport, adjacent to NDV (see Figure 2c), as provided by the National Climatic Data Center, were considered unreliable due to their significant inconsistency with other data sets in the area in terms of storm *magnitude*. However, the *timing* of events was generally consistent with the AZMET stations, which further supported the use of the AZMET rain data at NDV.

A comparison of the two AZMET data sets shows little difference in PET between the stations, suggesting that either data set would be appropriate for use at NDV. The Queen Creek site was chosen as the primary source because the nearby farms and suburban development were deemed analogous to the adjacent golf course and campus housing at NDV, as compared to the more densely developed area surrounding the Mesa AZMET station. Calculated using a simplified version of the Penman-Monteith Equation recommended by the American Society of Civil Engineers, the AZMET PET value is an appropriate estimate for evaporative demand and evapotranspiration in ecosystems with high water supply (Brown, 2005).

Two sensors recorded volumetric soil moisture hourly at each of the four NDV neighborhoods. Where applicable, the two sensors for each neighborhood were buried under areas of differing ground cover, as shown in Table 1. Unprocessed data showed volumetric soil moisture as high as $0.7480 \text{ m}^3/\text{m}^3$; such high values on a scale where the maximum value should equal porosity suggested that a sensor calibration was necessary. Since this precise maximum value was achieved multiple times at different locations, all soil moisture data was normalized to this value, thereby interpreting this sensor reading as a point of maximum saturation. Thus a sensor calibration was achieved simultaneously with a conversion from volumetric soil moisture to the dimensionless relative soil moisture (s) used in the model, without requiring an estimate for porosity, which instead is included in a calibration parameter as described below. After the conversion, daily soil moisture values were calculated as the arithmetic mean of each day's hourly data.

Figure 3 shows data (after normalization) from the xeric and mesic sites used for model calibrations, with precipitation and PET records from the Queen Creek AZMET station. The “irrigated” xeric sensor was placed under a palo verde tree instrumented with four drip-style irrigation emitters. The “non-irrigated” sensor was installed away from any vegetation (and thus irrigation) in an area covered only by a layer of granitic gravel. The sensor at the mesic site was under turf grass with a sprinkler irrigation system. Thus the irrigated sensor at the xeric site showed much higher soil moisture values than that at the mesic site due to the point source irrigation directly above it, as opposed to the spatially distributed irrigation at the mesic site. The lateral heterogeneity in irrigation at the xeric site suggests that despite higher soil moisture, the volume of water there can still be significantly less than at the mesic site, as would be expected.

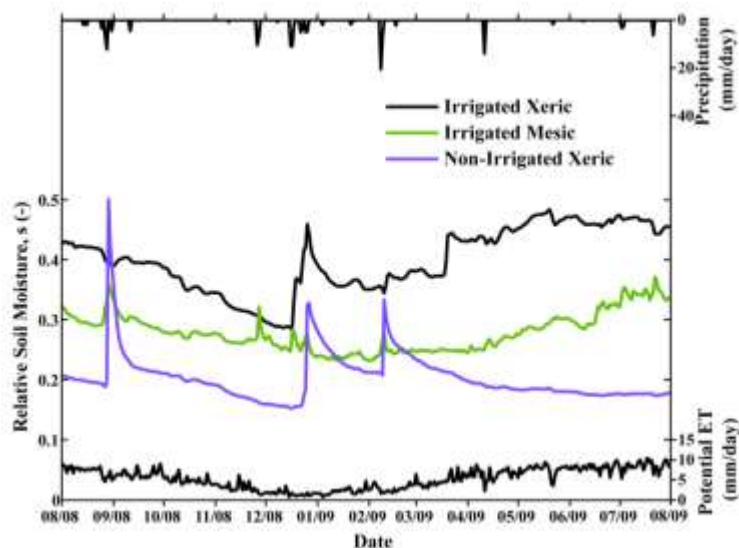


Figure 3. Data used for calibration, including meteorological forcing recorded at AZMet station in Queen Creek, as well as soil moisture data from three sensors at NDV.

It should be noted that while all three sensors recorded a response to large rain events in August, December, and February, the xeric sensors had no response to the November event. Additionally, the April event was not recorded at the non-irrigated sensor, and is difficult to discern at the irrigated sites. Finally, the relatively small August event appeared to have a disproportionately large effect at both sites when compared to the larger February event. These observations are the impetus for adjustments made to facilitate the calibration process as described below.

2.4 Calibration Routine and Procedures

Calibration Strategy

Using the meteorological data from the Queen Creek AZMET station as model forcing, an automated optimization routine was used to determine the necessary soil and vegetative parameters and thereby calibrate the model to the three NDV soil moisture time series shown in Figure 3. The Shuffled Complex Evolution (SCE) method developed by Duan *et al.* (1993) combines the optimization strategies of clustering, shuffled complexes, and competitive evolution to search multi-dimensional spaces for globally optimized parameter values. Our objective function was the minimization of the root mean square error (RMSE) between the observed and modeled soil moisture time series.

The model was calibrated to each of the three time series sequentially, in order to take advantage of parameters shared between sites and thereby increase computational efficiency and obtain the most reliable values conditions would allow. In order to test for parameter convergence and determine the relative dependence of the objective function on each parameter, up to 100 independent calibrations were performed for each time series, with each calibration consisting of approximately 20,000 model runs. Boundaries for the parameter space were chosen based on values from published literature (e.g. Caylor *et al.*, 2005; Laio *et al.*, 2001a, b; Manfreda *et al.*, 2010; Porporato *et al.*, 2003; Vico and Porporato, 2011), observed conditions, and estimates from preliminary manual calibration, though efforts were made to avoid confining the parameter space such that an optimal solution occurred along a boundary. Model validation was achieved using data from the same sensors during different time periods, though the limited duration of reliable data often necessitated shorter validation periods.

Non-Irrigated Model Calibration, Xeric Site

Since irrigation input represents a relatively unknown model forcing (discussed below), and in order to build confidence in the model, the non-irrigated xeric sensor was chosen as the first calibration exercise. Though this sensor is covered only by bare soil, allowing for an assumption of zero interception, it is expected that the surrounding vegetation at the xeric site nonetheless still has an impact on water dynamics through evapotranspiration of soil moisture. Preliminary tests indicated that soil moisture levels at the site were too low to induce significant deep infiltration beyond the rooting zone, so parameters used

in the model only in the calculation of leakage (s_{fc} , K_s , and b) were unable to converge to viable calibrated values. Since the model does not use porosity or the rooting depth independently, their product nZ_r was used as a calibration parameter; it is not possible to separate the two to independently determine either using this method of calibrating this model. Thus the set of model parameters determined in this initial calibration exercise includes nZ_r , s_h , s_w , s^* , and E_w . Of these, s_h and E_w are dependent on only soil properties and thus are applicable throughout NDV. nZ_r , s_w , and s^* are dependent on both soil and vegetation and therefore can be applied only within the xeric site. Antecedent moisture conditions were determined by calibrating a value for initial soil moisture s_0 .

The final calibrated parameter was the depth of the late August rain event, since the data suggest the precipitation record from Queen Creek may not appropriately represent rainfall at NDV for this event. The soil moisture series shows a disproportionately large increase compared to later rain events with more rainfall recorded at the Queen Creek station. While recreational activity by local residents may be a cause of soil moisture beyond that added by precipitation, spatial heterogeneity of summer storms in the region is likely the cause for the discrepancy. The Mesa AZMET station, for example, shows an event earlier that month consisting of several centimeters over three days, though no rainfall was reported at Queen Creek during that time. The August event thus lacks a reliably applicable rainfall depth, despite the importance of such a value due to the relative dominance of the effects of the wetting event on the late summer moisture time series. It was therefore decided to use the magnitude of the storm as a calibration parameter, thereby basing the calibration on the shape of the recession curves, and the more spatially homogeneous winter events with more consistent rainfall data and clear effects, rather than the uncertain summer storm. Similarly, the large November and April events seen at the AZMET station were also removed from the precipitation record, as there was clearly no record of them at the xeric site. In order for the model to achieve reasonable and reliable calibration results that accurately simulate the true soil moisture record, it was necessary to choose a rainfall record where major events are seen as corresponding peaks in the soil moisture record, regardless of the reason for the discrepancy between the rain data and the events seen by the moisture sensors.

Irrigated Model Calibrations: Xeric and Mesic Sites

Although monthly water meter readings were kept for the irrigation systems in each of the neighborhoods, undocumented changes to the irrigation schedule disallow temporal resolution of irrigation input into a unit amenable to the current numerical simulation. Furthermore, heterogeneities in distribution mechanisms and irrigation frequencies and durations make conversion from volumetric readings to irrigation depths problematic. Therefore, without reliably precise irrigation data, anthropogenic water input was modeled as an average daily addition to the meteorological forcing, varying on a monthly basis. Modeling irrigation application as a daily event alleviates issues of resolving an irrigation schedule from coarse data, while simultaneously accounting for the dissolution of the wetting front expected as water percolates through the rooting zone to the sensor depth. The observed data supports this essentially continuous treatment (water application at each time step), as individual irrigation pulses are seen in the soil record as small, frequent increases in moisture levels, resulting in a relatively smooth curve when compared to data influenced only by rainfall (see Figure 3). Additionally, these monthly irrigation parameters implicitly account for seasonally-dependent subtractions from water input due to interception.

To investigate the relative effects of different landscape and irrigation treatments, the model was calibrated using data from irrigated sensors at both the xeric and mesic sites. The second calibration exercise applied the parameters determined from the non-irrigated xeric sensor, with the same precipitation forcing, to data from the irrigated xeric sensor. This calibration provided monthly irrigation parameters for the xeric site, as well as the soil parameters used in the determination of leakage rates that were indiscernible from the non-irrigated sensor. In the final calibration exercise, parameters dependent only on soil properties (assumed constant throughout NDV) were maintained from the previous calibrations, but vegetation- and site-dependent parameters nZ_r , s_w , s^* , and s_0 were recalibrated with the monthly irrigation parameters for the mesic site. The magnitude of the August storm was recalibrated

again to account for spatial heterogeneity and emphasize the more reliable portions of the soil moisture time series. Also, as the April and November events were seen in the sensor data at the mesic site, they were reintroduced to the rainfall record for this calibration.

2.5 Experiments

To investigate the impact of varying irrigation schedules, the total annual irrigation inputs determined in the above calibrations were temporally redistributed according to four irrigation scenarios representative of those found in the Phoenix metropolitan area (see Figure 4). The first divides the annual total into equal daily inputs, representing daily irrigation without any seasonal variation. The second scenario provides daily input, while maintaining the seasonality (ratios between monthly irrigation values) determined in the calibration. The third and fourth scenarios are analogous to the first two, but deliver irrigation as monthly pulses, representing flood-style irrigation practices. The third scenario divides the annual input into twelve equal monthly pulses, while the fourth varies the pulse volume according to the monthly ratios determined in the calibration. All four scenarios use the same annual total irrigation input, varying only the distribution schedule.

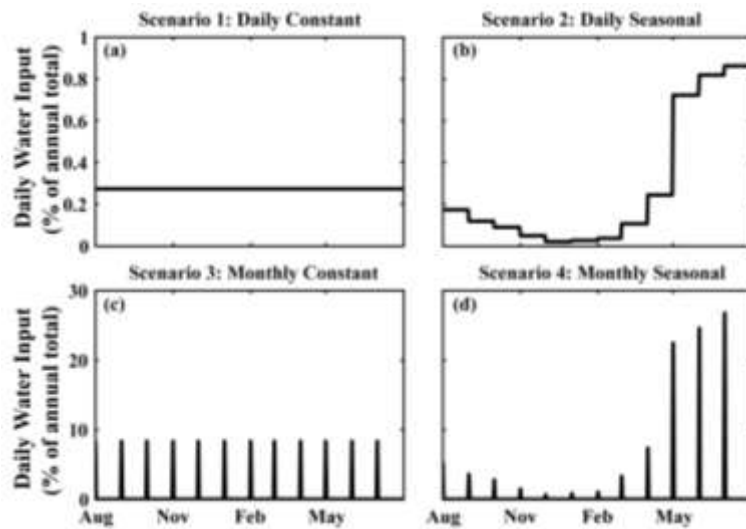


Figure 4. Examples of irrigation input for four experimental scenarios of varying frequency and seasonality. Daily irrigation (a and b) is compared to monthly pulses (c and d), and seasonally constant volumes (a and c) are compared to seasonal variations (b and d).

Simulations were run for a five-year period, using the calibrated model parameters from both the irrigated xeric and mesic sensors, with meteorological forcing data (precipitation and PET) from the AZMET stations. Soil moisture statistics were observed for the base case, representing the total annual irrigation determined in the calibration for each site. Simulations were then run using a range of annual irrigation totals in order to investigate the impact of varying irrigation volume on soil moisture statistics, water partitioning and plant water stress for all four scenarios at both sites. In these simulations, seasonality was maintained by keeping constant the percentage of annual irrigation applied during each month, effectively scaling water input by keeping month-to-month ratios the same. Plant water stress was also calculated with varying plant stress parameters, and under cases of inter- and intra-annual precipitation variability.

Finally, the SCE optimization routine was used to find irrigation schedules that achieved goal plant water stress values while minimizing water input. Monthly-varying daily irrigation input values were again determined, with an objective function that simultaneously minimized total annual input while maintaining the goal dynamic water stress value. For these simulations, 61 years of precipitation data from Phoenix Sky Harbor Airport (1950-2010, acquired through the National Climatic Data Center) were used to reflect inter-annual meteorological fluctuations. Other model parameters were maintained from the calibration exercises, and PET for each day of the year was taken as the average of values for that day among ten consecutive years of PET data from the AZMET Queen Creek site.

3. Results and Discussion

3.1 Model Calibrations

Xeric Site, Non-Irrigated Sensor

Table 2 shows the parameter limits used for the three calibrations, as well as values at which the objective function was optimized for each. Parameters marked with a “+” are dependent only on soil characteristics and are thus applied to other sites at NDV. Parameters with a “#” are dependent on vegetation as well, and are therefore only applied to the site at which they are calibrated. Additionally, the depth of the August storm event was calibrated at the non-irrigated xeric sensor to 67.8 mm, and at the mesic site to 47.1 mm. Antecedent moisture conditions were also determined by calibrating initial relative soil moisture to 0.202, 0.461, and 0.313 for the non-irrigated xeric, irrigated xeric, and irrigated mesic sites, respectively.

Table 2. Parameter values determined for the three model calibrations, with calibration range used for each.

Parameter	Units	Symbol	Lower Bound	Optimized Value	Upper Bound
<i>Xeric Site, Non-Irrigated</i>					
Porosity*Rooting Depth (#)	[mm]	nZ_r	20	347	3.2×10^3
Hygroscopic Point (+)	[-]	s_h	0	0.133	0.15
Wilting Point (#)	[-]	s_w	0.15	0.221	0.25
Stress Threshold (#)	[-]	s^*	0.25	0.310	0.45
Bare Soil Evaporation (+)	[mm/d]	E_w	0.01	0.347	0.40
<i>Xeric Site, Irrigated</i>					
Field Capacity (+)	[-]	s_{fc}	0.4	0.429	0.75
Pore Size Distribution Index (+)	[-]	b	1	2.54	10
Saturated Hydraulic Conductivity (+)	[mm/d]	K_s	1	1.94×10^3	1×10^4
<i>Mesic Site, Irrigated</i>					
Porosity*Rooting Depth	[mm]	nZ_r	20	2.0×10^3	3.2×10^3
Wilting Point	[-]	s_w	0.15	0.236	0.24
Stress Threshold	[-]	s^*	0.24	0.248	0.42

The results of the first calibration, utilizing data from the non-irrigated xeric sensor, are presented in Figure 5. The soil moisture time series shows an excellent visual fit between the model and observed data, and a low RMSE of 0.01713, building confidence in the use of this model at this location. Model validation used meteorological data from the same source over the 10 months following the calibration period, and resulted in an RMSE of 0.05233. Much of the difference between the two RMSE values is thought to be the result of differences between the rain record at the AZMet station and that which actually occurred at NDV.

Several features of the observed data corroborate various elements of the model physics. Most notably, the differences in the slope of the recession limbs at similar soil moisture values are explained by seasonally-dependent PET rates: less ET after the December storm results in a slower recession, while the February and August events are followed by increasingly higher PET rates and thus exhibit visibly steeper recession limbs at the same soil moisture value. The wilting point can be seen in the time series as the approximate soil moisture value (0.22) at which the slope of the recession limbs decreases significantly to a slower rate of moisture loss in the inter-storm periods. This slope below the wilting point is directly related to the bare soil evaporation rate, which had a calibrated value (0.347 mm/d) similar to, though higher than, that assumed by the model’s original authors (0.1 mm/d; Laio *et al.*, 2001b). The relatively large response to watering events (as compared to the mesic site, to be discussed

later) is accounted for in the model by a relatively low nZ_r value. This is to be expected since the majority of the xeric site is covered by bare soil, severely decreasing the average rooting depth in the area surrounding the sensors.

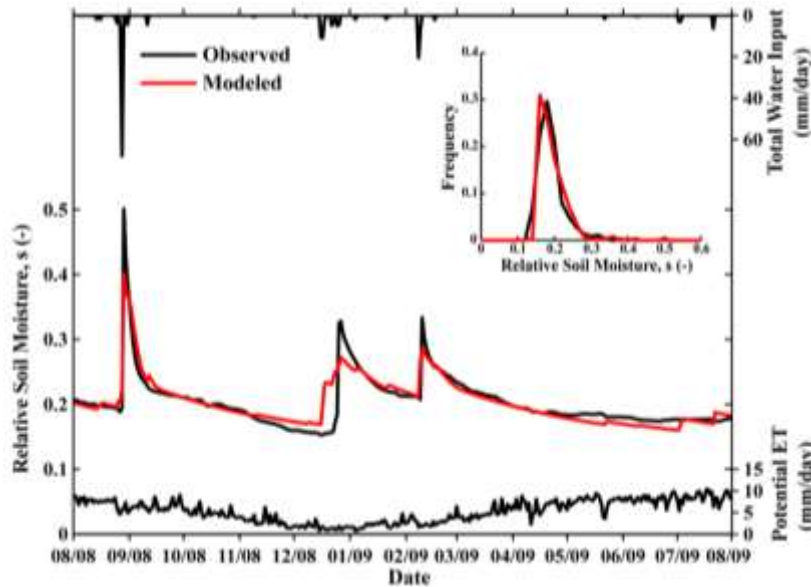


Figure 5. Results of calibration at non-irrigated xeric site. Calibrated parameter values are shown in Table 2. Precipitation record includes calibrated August event as discussed in text. Soil moisture values from the time series are shown as a frequency diagram in the inset, in which ordinate values represent frequency of soil moisture values within a bin interval of 0.02, relative to the total number of data points. Similar frequency diagrams are included in Figures 6, 7, and 8.

Xeric Site, Irrigated Sensor

Figure 6 shows the results of the second calibration, which utilized data from the irrigated xeric sensor and the calibrated parameters from the non-irrigated xeric sensor to determine irrigation rates and additional soil parameters, as reported in Table 2. The 12-month calibration period had an RMSE of 0.01659; a validation period of the preceding 7 months had an RMSE of 0.06725. The validation does not account for inter-annual variability in irrigation, which is thought to cause much of the difference between the two RMSE values.

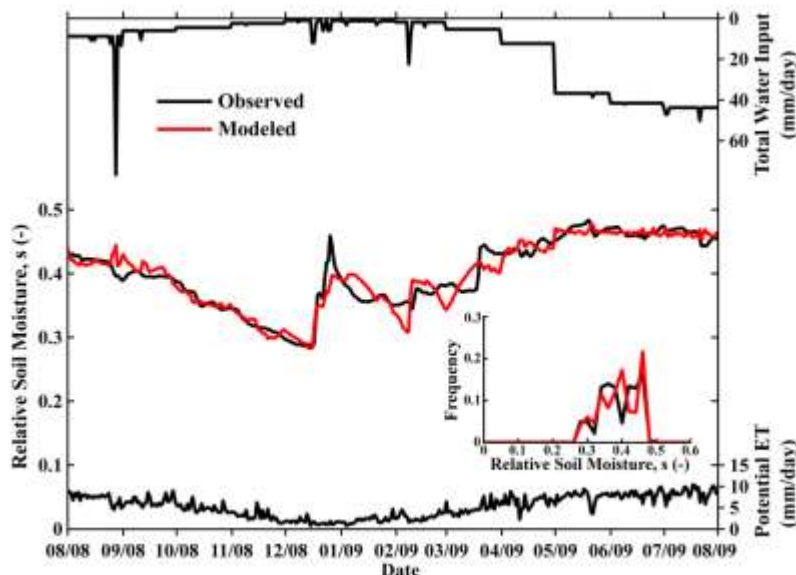


Figure 6. Results of calibration at irrigated xeric site. Soil moisture values from the time series in (a) are shown as a frequency diagram in (b). Water input includes same precipitation as at non-irrigated xeric site, plus calibrated daily irrigation. Other calibrated parameter values shown in Table 2.

The large response to the December storms (again, as compared to the mesic site), confirms the use of a low nZ_r value similar to the previous calibration. Excluding those wetting events, the soil moisture time series shows a sinusoidal trend that is synchronous with the trend in PET (higher values in summer). With constant irrigation, these trends would be asynchronous, as periods of high PET would result in lower soil moisture. Thus the observed data shows that the seasonality of irrigation rates (greater

in the summer, as is customary practice and supported by water meter readings, not presented) was sufficient to overcome the seasonal effects of ET rates. Calibrated values for s_{fc} , b , and K_s are reasonable compared to those used for similar soil types in other studies (e.g. Laio *et al.*, 2001b).

There are two factors contributing to the greater variability of the model results in this calibration as compared to the observed data, as exhibited visually in the time series. First, irrigation is modeled as varying at a monthly scale, resulting in abrupt changes in water input that are reflected in the soil moisture time series. While modeling irrigation rates with a finer resolution would alleviate some of this variability, the monthly scale was necessary to maintain computational efficiency, yet still sufficient to capture the seasonal trends being studied. Second, while daily fluctuations in PET would be tempered in both space and time at the sensor depth, the point-scale model is unable to distribute losses unevenly throughout the rooting zone profile. This limitation is manifested as variations in soil moisture that coincide with daily fluctuations in PET, and not necessarily with variations in the observed data. These fluctuations are not seen in the previous calibration because without irrigation input, the relative soil moisture values were closer to the wilting point, where ET is modeled at the invariant E_w rate, than to the stress threshold, where ET is modeled at the daily fluctuating PET rate. The effect of these fluctuations can also be seen in the frequency diagram in the inset of Figure 6. The model captures the range and peak of soil moisture frequency, but is unable to duplicate finer ranges of soil moisture in which observations were made more often.

Mesic Site (Irrigated)

As mentioned above, the soil moisture time series at the mesic site (Fig. 7) shows significantly smaller response to storm events than at the xeric site, due to the significantly larger average rooting depth. The calibrated water input in Figure 7 shows seasonality similar to the xeric site, though the values are substantially smaller. Though it may seem counterintuitive that the high water-use turf grass receives less irrigation than the xeric site, comprised of low water use plants and bare gravel, differences in the method of irrigation must be considered. The drip irrigators at the xeric site concentrate water input at plant locations with a small wetting perimeter, resulting in greater values of irrigation *depth* without a necessarily similar relationship in irrigation *volume*. Similarly, moisture levels are significantly lower at the mesic than at the irrigated xeric sensor, though this may only suggest that the high water use plants are transpiring more. This, however, could also be the result of a better balance between ET losses and irrigation input, a balance that would be easier to achieve with the larger storage capacity afforded by the increased rooting depth, and further suggested by the smaller distribution of soil moisture values throughout the year. While the reported value for the wilting point (0.236) is close to the boundary of the parameter space (0.240), the optimized parameter value did not approach the bound, and instead remained under 0.237 for independent calibrations. Similarly, the stress threshold converged to values (0.248) significantly greater than the lower bound on that parameter (also 0.240). Thus, the difference between the two threshold values is relatively small, but the precision of the optimization ensures a positive space between them, which is then magnified in volumetric terms by the relatively large rooting depth. The RMSE for the calibration was 0.00940, with a validation RMSE in the following ten months of 0.03890. Differences are thought to be primarily the result of inter-annual fluctuations in irrigation input, similar to the irrigated xeric site.

The observed data at the mesic site show several independent peaks that do not correspond to storm events in the rainfall record, particularly in late 2008. These are likely to instead be the result of irrigation events, which are being modeled as smaller daily inputs. Since the model is unable to capture these events, the optimization routine searches the parameter space to minimize their effect, which hinders its ability to model actual rain events. Nonetheless, the model is able to simulate average soil moisture values very well, as shown by the visual fit, the RMSE, and the frequency diagram, which are all comparable across the three calibrations. Still, the results of the calibrations should not be seen as precise determinations of site properties and water input; rather, they serve only as a basis for an analysis of general trends and monthly/seasonal averages, and for the following comparison between the two sites.

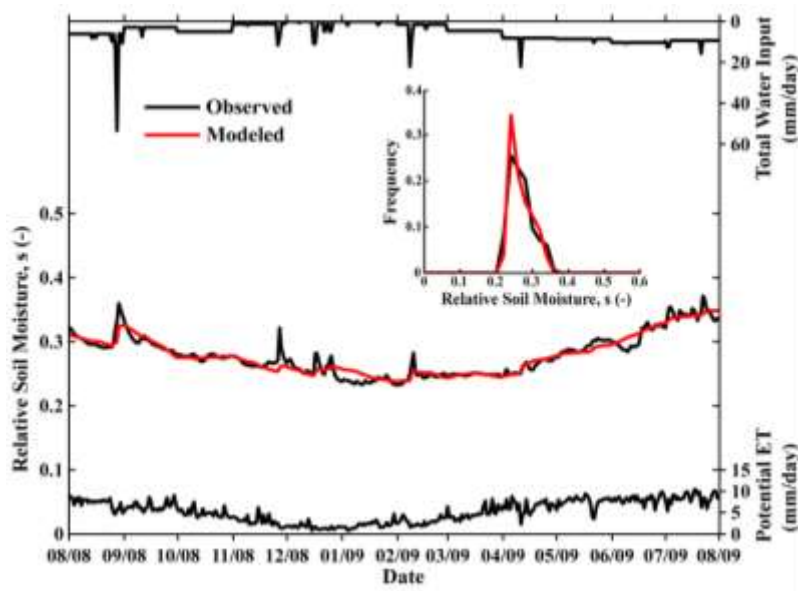


Figure 7. Results of calibration at irrigated mesic site. Soil moisture values from the time series in (a) are shown as a frequency diagram in (b). Water input includes recalibrated depth of August event, and daily irrigation input. Other calibrated parameters shown in Table 2.

3.2 Irrigation Experiments

Figure 8 shows frequencies of modeled soil moisture values at the two irrigated sites using the calibrated parameter values from Table 2 and five years of historical rainfall and ET data. Irrigation was included using annual totals derived from the calibrations, distributed according to the four scenarios outlined earlier and in Figure 4, with the same seasonality as determined in the calibrations. At the xeric site, infrequent applications of large water volumes are unable to maintain soil moisture values above the wilting point of 0.22, regardless of the seasonality of irrigation input. The same annual input temporally distributed at a daily scale resulted in much higher soil moisture values. This difference is due to the shallow rooting depth at the xeric site, creating a lack of available storage for the large monthly pulses. Daily irrigation that is constant throughout the year maintained relatively constant soil moisture near the field capacity of the soil (87% of days, $s \geq 0.44$; 0% $s \leq 0.40$). Seasonal irrigation resulted in more variable soil moisture (34% of days, $s \geq 0.44$; 30% $s \leq 0.40$), though there were still no days with moisture below the wilting point. The significant time above field capacity suggests large losses to deep infiltration beyond the rooting zone, which may be avoided by lower soil moisture values with seasonal irrigation.

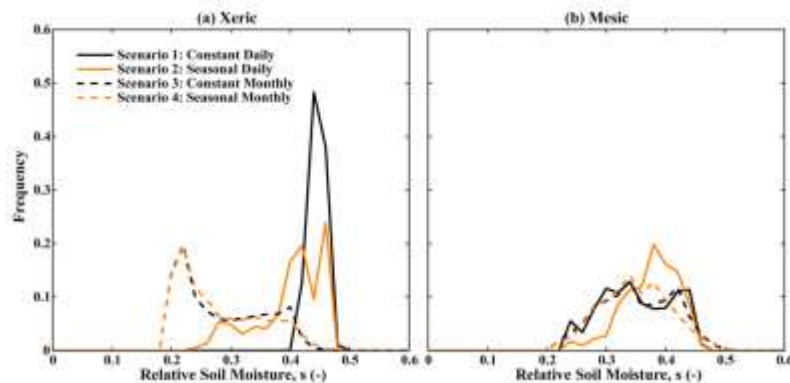


Figure 8. Frequency diagrams of soil moisture using calibrated model, five years of historical meteorological forcing data (January 2006 – December 2010), and irrigation scenarios 1-4 (illustrated in Figure 4) at irrigated xeric (a) and mesic (b) sites. Consistent with other frequency diagrams in Figures 5, 6, and 7, ordinate values represent frequency of soil moisture values within a bin interval of 0.02, relative to the total number of data points.

For each of the four irrigation scenarios, the frequency of soil moisture values is more evenly distributed across the range of achieved values at the mesic site than at the xeric. This is likely because the greater storage capacity of the larger rooting depth can act as a buffer against changes in irrigation and meteorological conditions. This results in relatively small daily changes in relative soil moisture with less influence from threshold values such as the wilting point, where transpiration is suspended, and the field capacity, at which leakage is induced.

While the average soil moisture at the mesic site is comparable among all four irrigation scenarios (0.361, 0.385, 0.362, and 0.359 respectively), there are noteworthy differences in the distribution of the data. Scenario 1 exhibits bimodality at the mesic site, with high soil moisture values being attained in the winter months due to irrigation in excess of potential evapotranspiration, and low values in the summers when irrigation is insufficient to compensate for the increased rate of PET. However, scenario 2 shows a slightly narrower and more normal distribution, with a greater average value than the other three scenarios. The monthly scenarios show wider distributions than their daily counterparts, both in terms of range and standard deviation. The moisture deficits occur during summer months immediately before an irrigation pulse, the surpluses in winter months on dates when pulses are delivered. The bimodality seen in scenario 1 is also exhibited in scenario 3, and for similar reasons, while scenario 4 has a more normal distribution, with a slightly lower average value.

The results of varying total annual irrigation input in each of the four scenarios are shown in Figures 9 (soil moisture statistics) and 10 (water partitioning). At the xeric site, infrequent application of large irrigation pulses (scenarios 3 and 4) shows no advantage over daily irrigation in terms of average soil moisture. For low irrigation, effects of monthly irrigation match those of daily input, but since the shallow soil profile (low nZ_r) limits the capacity to store water from the monthly pulses, additional water input has no affect. Additionally, for annual irrigation greater than approximately 2000 mm, at least 60% of water input is lost to either runoff or leak.

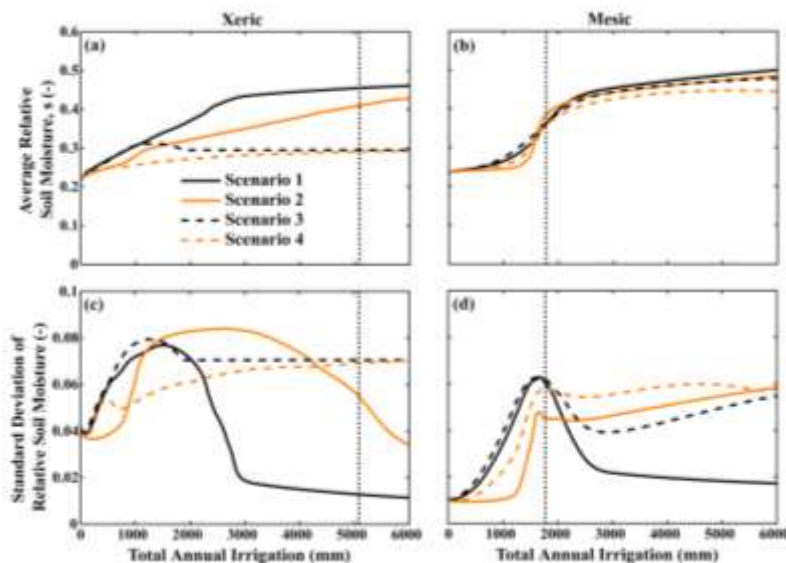


Figure 9. Soil moisture statistics for varying total annual irrigation depths using calibrated model at xeric (a, c) and mesic (b, d) sites. Dotted vertical line indicates base input from calibrations.

However, far better results are achieved with daily irrigation at the xeric site (scenarios 1 and 2). While approximately 35% of water is lost to deep infiltration and runoff using the base (calibrated) water input (and an even higher percentage with greater input), less irrigation can substantially decrease and even virtually eliminate these losses. In particular, for irrigation input between 200 and 1000 mm, approximately 80% of water in scenario 2 is utilized as stressed ET. In this range, average soil moisture is only marginally lower with seasonal than with invariant irrigation, but the variation in soil moisture is much lower and leak is eliminated. Thus, by balancing seasonal trends in PET with a corresponding irrigation schedule, soil moisture values can be maintained in a range that minimizes ET without falling below the wilting point. For annual input greater than 1000 mm, average soil moisture continues to increase while variability eventually decreases, but more water is lost to deep infiltration and plants are transpiring at the maximum potential rate.

At the mesic site, all four scenarios showed similar behavior with increasing irrigation input. Between 500 and 1500 mm of annual input, monthly irrigation provides slightly higher average soil moisture, with seasonality having a larger impact than frequency. However, for irrigation input greater than 2000 mm, frequency of input appears to be the dominant parameter, with slightly higher average soil

moisture under daily irrigation. Variability in soil moisture was lower in seasonal scenarios than invariant ones for low irrigation volumes, as irrigation patterns better matched patterns of losses through ET. This relationship eventually reverses with more applied water as the variable input overcompensates for the annual pattern in ET. Monthly irrigation consistently results in greater variability in soil moisture, as seen in Figure 8 and discussed above. In terms of water partitioning for small amounts of irrigation, this translates to more unstressed ET above the stress threshold, but also more evaporation below the wilting point. With more irrigation input, leakage losses increase from the small percentage at the base (calibrated) irrigation volume, though significant runoff losses were not triggered in the range tested.

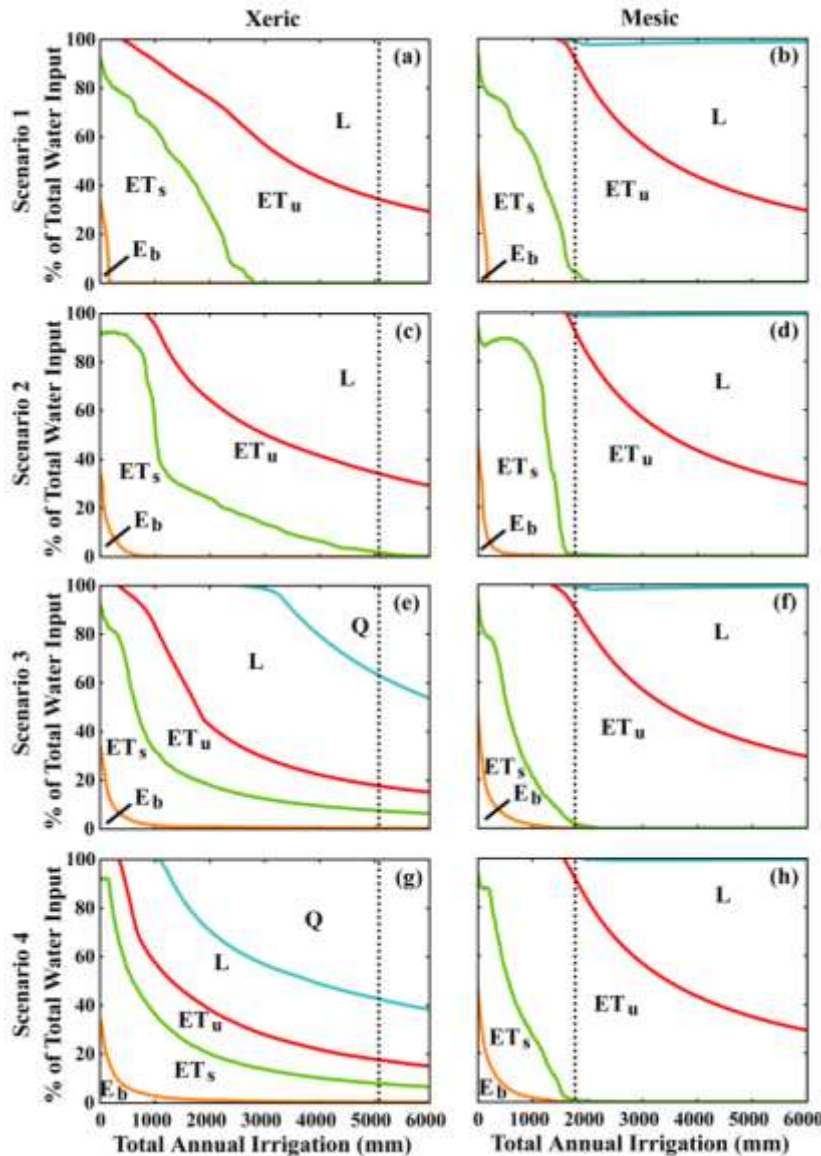


Figure 10. Partitioning of total water input for varying total annual irrigation depths at xeric (a, c, e, g) and mesic (b, d, f, h) sites using scenarios 1 (a, b), 2 (c, d), 3 (e, f), and 4 (g, h). Dotted vertical line indicates base input from calibrations. Q = runoff ($s > 1$), L = deep infiltration (leak) ($s_{fc} < s < 1$), ET_u = unstressed evapotranspiration ($s^* < s < s_{fc}$), ET_s = stressed evapotranspiration ($s_w < s < s^*$), E_b = bare soil evaporation ($s < s_w$). Dotted vertical line indicates base input from calibrations.

3.3 Plant Water Stress

Figure 11 shows, for both irrigated sites, trends in plant water stress as a function of irrigation scenario, water input volume, and plant resilience parameters q and k . Soil moisture values between the wilting point and the stress threshold, in which ET increases from the bare soil evaporation to the maximum rate, were chosen as a goal because this range maintains some plant water stress without inducing wilting effects. For non-agricultural purposes, a limited amount of water stress is thought to be advantageous by decreasing production of biomass, and thereby reducing required maintenance, in addition to water savings achieved by keeping plants slightly thirsty.

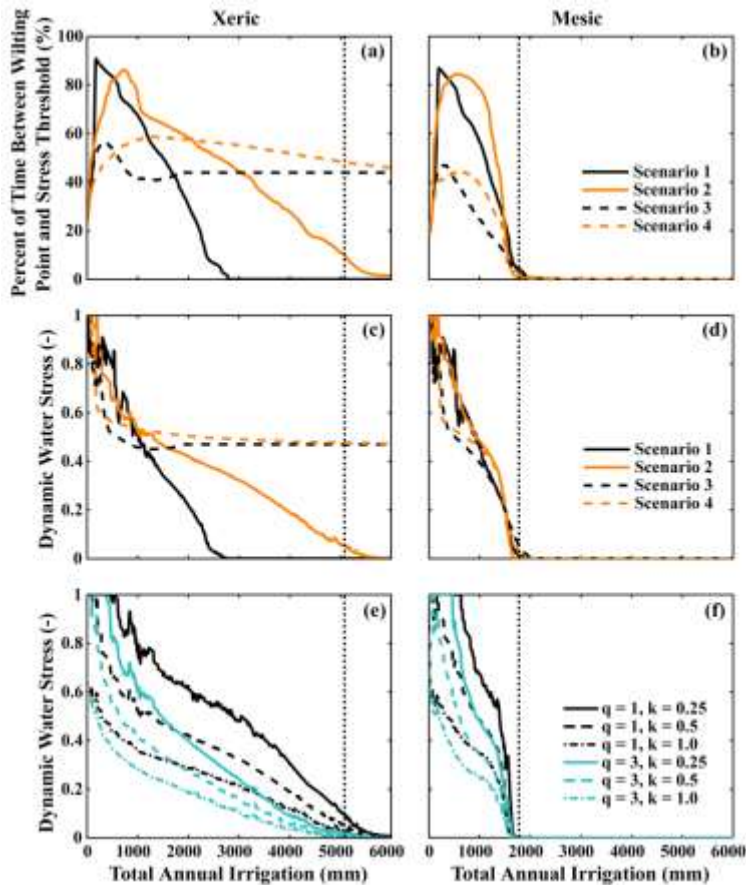


Figure 11. Stress diagrams for xeric (a, c, e) and mesic (b, d, f) sites. (a) and (b) show the percentage of time with stressed ET ($s_w < s < s^*$) for all four scenarios. This range was chosen as a goal to minimize both plant damage and water use. (c) and (d) show average dynamic water stress for a year-long growing season (1 = permanent damage; $q = 1, k = 0.5$). (e) and (f) show, for scenario 2 at each site, average dynamic water stress for several combinations of k and q values. Other scenarios, not pictured, show similar effects. Noise in dynamic stress plots is due to discrete counts in the dynamic stress function, particularly in the exponent. Dotted vertical line indicates base input from calibrations.

At both sites, daily irrigation provides high percentages of time (60 - 90%) within the goal range for annual irrigation between 200 and 1000 mm; this is consistent with the high values for stressed ET shown in Figure 10. These percentages decrease as more water is added, keeping soil moisture levels above the stress threshold more often. Monthly irrigation achieves lower percentages in the goal range at the mesic site, similarly decreasing with increasing irrigation, though the limited storage capacity of the xeric site prevents improved conditions with additional water provided in monthly pulses.

Varying seasonality at the mesic site shows little impact in dynamic water stress, but seasonal irrigation at the xeric site results in substantially higher stress values. This suggests that monthly ratios should be adjusted to redistribute annual input and better compensate for losses to ET , as discussed below. Nonetheless, a decrease in irrigation at the xeric site to approximately 1500 mm/yr could maintain dynamic water stress below 0.5 while reducing losses to leak in scenarios 1 and 2. At the mesic site, a substantial increase in dynamic water stress should be expected for any decrease in irrigation input under any scenario. However, if a dynamic water stress level of approximately 0.5 or greater is deemed acceptable, water savings of approximately 500 mm/yr could be achieved by using a monthly schedule as compared to a daily irrigation.

The two bottom panels show that for low levels of irrigation (< 500 mm), a plant's elasticity in response to water stress (q) and capacity to withstand prolonged stressed conditions (k) have similar effects on dynamic water stress between the two sites. The effects however, are significant, as plants well adapted to water stress (high q and k values) maintain moderate values for dynamic water stress even with no irrigation, while poorly adapted plants experience permanent damage even with as much as 600 mm/yr of irrigation. At the mesic site, the curves quickly converge as water stress is eliminated through increased irrigation. However, at the xeric site, plant characteristics (particularly elasticity q) can still have a substantial impact moderating the effects of water shortages. In other words, a reduction in irrigation from the base value will substantially increase plant water stress at the mesic site regardless of plant

characteristics, but the impact at the xeric site will largely depend on q and k values. Thus, while plant characteristics are important for moderating water stress under low irrigation at both sites, their importance dwindles as irrigation increases at the mesic site while still having a significant impact at the xeric site.

While this analysis has, to this point, considered the impacts of varying water input through irrigation, attention has yet to be given to variations in water input through changes in precipitation. Table 3 shows rainfall totals from six years recorded at Phoenix Sky Harbor Airport. To test the effects of inter-annual fluctuations, three years were chosen with widely varying annual precipitation totals, but similar percentages of annual rainfall in the summer months (April-September). Three years with similar totals but varying percentages of summer rain were chosen to show the effects of intra-annual variability in rainfall. Dynamic water stress for each of the six years at both sites is shown in Figure 12 as a function of irrigation input. The figure assumes daily irrigation, seasonally varied, with q and k values of 1 and 0.5, respectively.

Table 3. Precipitation data for years depicted in Figure 12. Summer months include the typically dry spring (April-June), plus the summer monsoon months (July-September).

Year	Winter Rain (mm)	Summer Rain (mm)	Total Rain (mm)	% of Total Rain During Summer
2009	50	33	83	40
1974	130	78	208	38
1992	213	149	362	41
1957	133	60	193	31
1958	97	110	207	53
1990	64	133	197	68

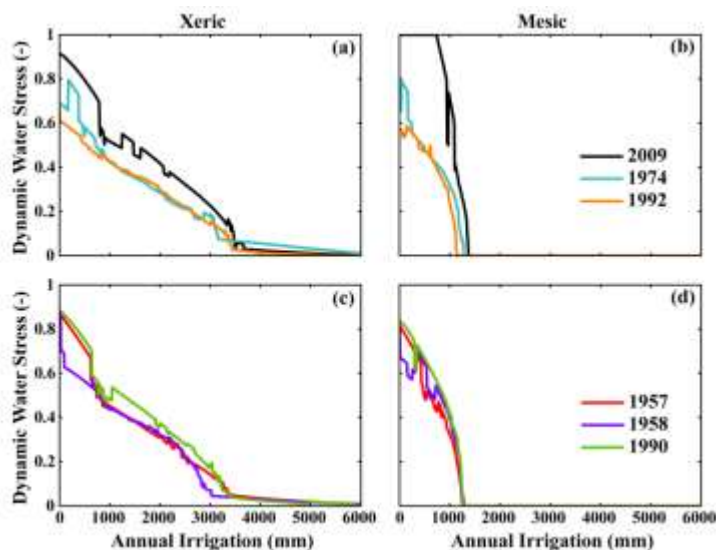


Figure 12. Effects of varying precipitation total and seasonality on dynamic water stress for different irrigation volumes and scenario 2 irrigation schedule. (a) and (b) compare years with varying precipitation totals but similar seasonality. (c) and (d) compare years with similar annual totals but different seasonality. Precipitation values shown in Table 4. Irrigation scenario 2 used, with assumed values for q and k of 1 and 0.5, respectively.

As expected, years with greater rainfall experienced lower levels of plant water stress, and with enough irrigation, differences in rainfall become inconsequential. However, the difference is more pronounced at the mesic site, suggesting that plants at the xeric site may incur less permanent damage in a dry year than those at the mesic site. This is likely due to plant-dependent characteristics such as the wilting point and stress threshold that are better suited to dry conditions. Differences in seasonality also decrease with increasing irrigation, but at both sites, years with highly seasonal rainfall showed greater plant water stress than the year with more evenly distributed rainfall. In fact, the effects of a year with

highly seasonal rainfall are comparable to those of a generally dry year at the xeric site. Additionally, increased irrigation causes faster convergence with intra-annual than inter-annual variability. These suggest that frequent application may be more important at the xeric site than the mesic, which again is likely a result of the difference in storage capacity in the rooting zone.

Figure 11(c) implies that for annual irrigation greater than 1000 mm at the xeric site, constant irrigation results in less dynamic water stress than seasonally varying irrigation. This is because the seasonality was determined in the calibrations and held constant. By varying monthly percentages, dynamic water stress should be improved, with constant irrigation representing a worst-case scenario where no advantages are gained by adjusting the annual schedule. Figure 13 shows the results of minimizing irrigation input while maintaining a given dynamic water stress value for both cases of daily water application. Annual irrigation values were much lower than the calibrated irrigation at the xeric site and comparable at the mesic site, which was anticipated from the soil moisture values (Figures 3 and 8), percentage of leak (Figure 10), and stress diagrams (Figure 11).

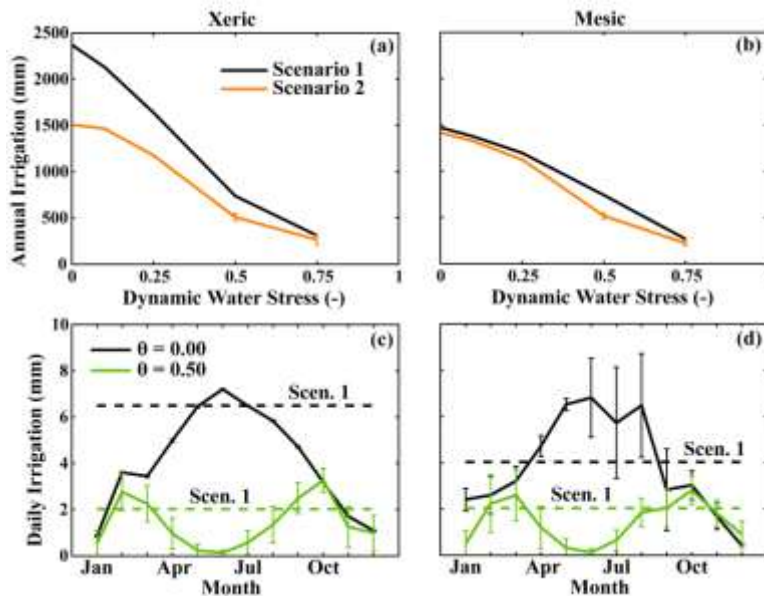


Figure 13. Minimal annual irrigation necessary to achieve goal values of dynamic water stress at xeric (a) and mesic (b) sites under scenarios 1 and 2 ($q = 1$; $k = 0.5$). (c) and (d) show irrigation schedule according to scenario 2 (solid lines) and scenario 1 (dashed lines) necessary to achieve goal dynamic water stress values while minimizing water input. Error bars show +/- one standard deviation from several independent optimization exercises.

The advantages of seasonal irrigation decrease as the acceptable water stress increases, which makes sense given that the extreme case of $\theta = 1$ would show no irrigation under either scenario. The mesic site, however, additionally shows limited advantage to seasonal irrigation when the stress tolerance is very low. Since the low tolerance requires soil moisture levels at or near the stress threshold, irrigation should essentially be merely compensating for losses to ET. The greater storage capacity allows the mesic site to hold excess water input in the winter months for use in the summer, whereas at the xeric site, the rooting zone cannot hold enough water to sustain the area through the summer. Furthermore, as the constraint of low stress is relaxed, opportunities for water savings with varying irrigation increase, until both scenarios converge again under high stress.

As expected, low stress tolerance requires considerably higher irrigation during the summer months, with the mesic site showing more variability due to its greater storage capacity. This is particularly true in summer months when water in storage is at a minimum: since soil moisture levels are being maintained at the stress threshold, ET rates are constant, but there is little risk of inducing leakage, allowing substantially variability in timing of application. Water can either be applied early and stored, or applied to match ET rates, with no difference in losses to either ET or leakage. This same reasoning further supports the use of less frequent irrigation schedules at the mesic site.

Interestingly, the optimized schedule with a high stress tolerance dictates a decrease in input during the winter to match reduced ET rates, but also prescribes a decrease in the summer months when more of the applied water would be lost to ET. Only enough water is allowed to enable the plants to

survive the summer near the wilting point, thereby achieving the tolerable stress level, then enough water is applied in the rest of the year to live closer to the stress threshold. These results are thought to be highly dependent on stress parameters q and k .

4. Summary and Conclusions

The point-scale model of soil moisture dynamics was able to adequately capture the recession curves at the non-irrigated xeric site, using historical records of daily precipitation and potential evapotranspiration rates. Differences among the recession limbs support the use of a model with seasonally varying rates of PET, an addition made here to the originally published model. Using several site-specific parameters calibrated to the non-irrigated soil moisture time series, including the depth of the spatially heterogeneous summer storm, an irrigated time series from the same xeric site was also calibrated: daily irrigation values were added to optimally match the observed soil moisture record. A similar process was applied to data from an irrigated sensor at the mesic site, which showed a greater storage capacity in the rooting zone, and, in terms of relative soil moisture, a smaller difference between the stress threshold and wilting point. The greater rooting depth at the mesic site is supported by the smaller range of soil moisture values, and the smaller response to wetting events

Annual irrigation totals from the calibrations were then used to investigate the impacts of irrigation scheduling at the two sites. The low storage capacity at the xeric site requires frequent irrigation to avoid large losses to runoff and leakage. For irrigation totals determined by the optimization, seasonal variation in input shows little benefit, but with less annual input, seasonal irrigation patterns better maintain soil moisture values between the stress threshold and wilting point. The mesic site shows bimodality in soil moisture for constant irrigation, with seasonal patterns resulting in a more normal distribution. Average soil moisture is highest with daily, seasonal irrigation at the calibrated irrigation amount, though relatively small changes in total annual input result in other scenarios having higher average values, with all four showing similar general trends. It therefore appears that proper scheduling of irrigation input is more important at the xeric site than at the mesic, in order to minimize water losses while maintaining optimal soil moisture ranges.

By calculating values of dynamic water stress for varying irrigation amounts, it was determined that both sites could withstand decreases in irrigation input if a given level of water stress is deemed acceptable. At the xeric site, substantial water savings could be achieved in either scenario with daily water input, by decreasing water losses to deep infiltration beyond the rooting zone. At the mesic site, stress values increase quickly with decreasing irrigation, though advantages may be gained using monthly irrigation. Plant stress parameters have a large impact on stress values for a given irrigation amount and schedule, particularly for low irrigation, and at the xeric site.

As expected, increased irrigation eliminates the impact on plant stress of inter- and intra-annual variability in precipitation, though for low irrigation, inter-annual differences in rainfall have a smaller effect at the xeric site than at the mesic site. The mesic site shows little variation in stress due to seasonality of rainfall, though the effects can be substantial at the xeric site, due to the smaller storage capacity afforded by the smaller rooting zone.

By adjusting month-to-month ratios of irrigation using site and vegetative parameters from the calibrations, a daily irrigation schedule was determined that minimizes water input while achieving a goal stress level, based on several decades of meteorological data. Again, the xeric site shows greater potential for water savings through seasonally varying irrigation, as compared with the mesic site, due to differences in storage capacity. For low stress tolerance, daily irrigation ranged from < 1 mm/d in the winter months to approximately 8 mm/d in the summer at both site, though the mesic site allowed for greater variability. For high stress tolerance, optimized water input shows a semi-annual cycle, with less water applied in both the summer (allowing for high stress levels when PET is very high) and the winter (maintaining low stress levels without excess input when PET is very low). This type of analysis, used to

minimize water input to urban landscapes in dry climates, is absolutely dependent on a model of soil moisture dynamics that includes seasonal fluctuations in PET.

While this analysis admittedly excludes model features such as sub-daily resolution of water fluxes, vertically heterogeneous distribution of soil moisture within the rooting zone, and dynamic vegetative processes, it nonetheless provides a comparison of soil moisture dynamics and plant water stress between two common urban landscape design options. For low water stress tolerance, seasonal variation in irrigation is of much greater importance at the xeric site than the mesic site in order to avoid leakage losses. However, less frequent and larger applications of irrigation input can have benefits at the mesic site, whereas the large water pulses would only contribute to runoff at the xeric site. Greater water savings through seasonal variation can be achieved at the mesic site with a higher stress tolerance, though it may prove beneficial to decrease water input in both summer and winter months while providing additional water during fall and spring.

Acknowledgments

Funding for this study has been received from the National Science Foundation, grants EF1049251: “Assessing Decadal Climate Change Impacts on Urban Populations in the Southwestern United States” and BCS-1026865 “Central Arizona-Phoenix Long-Term Ecological Research.”

References

- Balling Jr RC, Gober P. 2007. Climate variability and residential water use in the city of Phoenix, Arizona. *Journal of Applied Meteorology and Climatology* **46**: 1130-1137. DOI: 10.1175/JAM2518.1
- Balling Jr RC, Gober, P, Jones N. 2008. Sensitivity of residential water consumption to variations in climate: An intraurban analysis of Phoenix, Arizona. *Water Resources Research* **44**: W10401. DOI: 10.1029/2007WR006722
- Brown PW. 2005. Standard reference evapotranspiration: A new procedure for estimating reference evapotranspiration in Arizona. Cooperative Extension Publication AZ1324, University of Arizona, Tucson.
- Caylor KK, Manfreda S, Rodriguez-Iturbe I. 2005. On the coupled geomorphological and ecohydrological organization of river basins. *Advances in Water Resources* **28**: 69-86. DOI: 10.1016/j.advwatres.2004.08.013
- Chow WTL, Brazel AJ. 2012. Assessing xeriscaping as a sustainable heat island mitigation approach for a desert city. *Building and Environment* **47**: 170-181. DOI: 10.1016/j.buildenv.2011.070.27
- Clapp RB, Hornberger GM. 1978. Empirical equations for some soil hydraulic properties. *Water Resources Research* **14**: 601-604.
- Duan QY, Gupta VK, Sorooshian S. 1993. Shuffled complex evolution approach for effective and efficient global minimization. *Journal of Optimization Theory and Applications* **76**: 501-521. DOI: 10.1007/BG00939380
- Grimmond CSB, Roth M, Oke TR, Au YC, Best M, Betts R, Carmichael G, Cleugh H, Dabberdt W, Emmanuel R, Freitas E, Fortuniak K, Hanna S, Klein P, Kalkstein LS, Liu CH, Nickson A, Pearlmutter D, Sailor D, Voogt J. 2010. Climate and more sustainable cities: climate information for improved planning and management of cities (producers/capabilities perspective). *Procedia Environmental Sciences* **1**: 247-274. DOI: 10.1016/j.proenv.2010.09.016
- Jacobs K, Holway J. 2004. Managing for sustainability in an arid climate: Lessons learned from 20 years of groundwater management in Arizona. *Hydrogeology Journal* **12**: 52-65. DOI: 10.1007/s10040-003-0308-y
- King EG, Caylor KK. 2011. Ecohydrology in practice: strengths, conveniences, and opportunities. *Ecohydrology* **4**: 608-612. DOI: 10.1002/eco.248
- Laio F, Porporato A, Fernandez-Illescas CP, Rodriguez-Iturbe I. 2001a. Plants in water-controlled ecosystems: active role in hydrologic processes and response to water stress IV. Discussion of real cases. *Advances in Water Resources* **24**: 745-762.
- Laio F, Porporato A, Ridolfi L, Rodriguez-Iturbe I. 2001b. Plants in water-controlled ecosystems: active role in hydrologic processes and response to water stress II. Probabilistic soil moisture dynamics. *Advances in Water Resources* **24**: 707-723.
- Laio F, Porporato A, Ridolfi L, Rodriguez-Iturbe I. 2002. On the seasonal dynamics of mean soil moisture. *Journal of Geophysical Research* **107**: D15, 4272. DOI: 10.1029/2001JD001252
- Larson KL, Casagrande D, Harlan SL, Yabiku ST. 2009. Residents' yard choices and rationales in a desert city: Social priorities, ecological impacts, and decision tradeoffs. *Environmental Management* **44**: 921-937. DOI: 10.1007/s00267-009-9353-1.
- Manfreda S, Scanlon TM, Caylor KK. 2010. On the importance of accurate depiction of infiltration processes on modeled soil moisture and vegetation water stress. *Ecohydrology* **3**: 155-165. DOI: 10.1002/eco.79.
- Martin, CA. 2001. Landscape water use in Phoenix, Arizona. *Desert Plants* **17**: 26-31.
- Marin, CA. 2008. Landscape sustainability in a Sonoran Desert city. *Cities and the Environment* **1**(2): 1-16.
- Mayer PW, DeOreo WB (Eds.). 1999. *Residential End Uses of Water*. American Water Works Association Research Foundation: Denver, CO.
- McCarthy HR, Pataki DE. 2010. Drivers of variability in water use of native and non-native urban trees in the greater Los Angeles area. *Urban Ecosystems* **13**: 393-414. DOI: 10.1007/s11252-010-0127-6

- Mitchell VG, Cleugh HA, Grimmond CSB, Xu J. 2008. Linking urban water balance and energy balance models to analyse urban design options. *Hydrological Processes* **22**: 2891-2900. DOI: 10.1002/hyp.6868
- Pataki DE, Boone CG, Hogue TS, Jenerette GD, McFadden JP, Pincetl S. 2011. Socio-ecohydrology and the urban water challenge. *Ecohydrology* **4**: 341-347. DOI: 10.1002/eco.209
- Porporato A, Laio F, Ridolfi L, Caylor KK, Rodriguez-Iturbe I. 2003. Soil moisture and plant stress dynamics along the Kalahari precipitation gradient. *Journal of Geophysical Research* **108(D3)**: 4127. DOI: 10.1029/2002JD002448.
- Porporato A, Laio F, Ridolfi L, Rodriguez-Iturbe I. 2001. Plants in water-controlled ecosystems: active role in hydrologic processes and response to water stress III. Vegetation water stress. *Advances in Water Resources* **24**: 725-744.
- Rodriguez-Iturbe I, Porporato A. 2004. *Ecohydrology of Water-Controlled Ecosystems: Soil Moisture and Plant Dynamics*. Cambridge University.
- Rodriguez-Iturbe I, Porporato A, Laio F, Ridolfi, L. 2001. Plants in water-controlled ecosystems: active role in hydrologic processes and response to water stress I. Scope and general outline. *Advances in Water Resources* **24**: 695-705.
- Vico G, Porporato A. 2011. From rainfed agriculture to stress-avoidance irrigation: II. Sustainability, crop yield, and profitability. *Advances in Water Resources* **34**: 272-281. DOI: 10.1016/j.advwatres.2010.11.011.
- White R, Havlak R, Nations J, Pannkuk T, Thomas J, Chalmers D, Dewey D. 2004. *How Much Water is Enough? Using PET to Develop Water Budgets for Residential Landscapes*. Texas Water Resources Institute: College Station, TX.
- Yabiku ST, Casagrande DG, Farley-Metzger E. 2008. Preferences for landscape choice in a Southwestern desert city. *Environment and Behavior* **40**: 382-400. DOI: 10.1177/0013916507300359